Published in final edited form as:
J Org Chem. 2013 April 5; 78(7): . doi:10.1021/jo400101d.

Pushing the Boundaries of Intrinsically Stable Radicals: Inverse Design using the Thiadiazinyl Radical as a Template

Freija De Vleeschouwer[1], **Artiom Chankisjijev**[1], **Weitao Yang**[2], **Paul Geerlings**[1], and **Frank De Proft**[1]

Freija De Vleeschouwer: fdevlees@vub.ac.be

[1]Eenheid Algemene Chemie (ALGC), Vrije Universiteit Brussel (VUB), Pleinlaan 2, B-1050 Brussels, Belgium

[2]Department of Chemistry, Duke University, Durham, North Carolina 27708, USA

Abstract

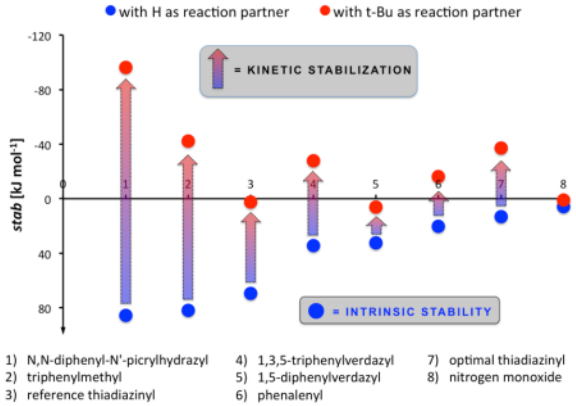

In this study, for the first time inverse design was applied to search for the intrinsically most stable radical system in a predefined chemical space of enormous size by scanning in a rational way that entire chemical space. The focus lied predominantly on thermodynamic stabilization effects, like stabilization through resonance. Two different properties were optimized: a newly introduced descriptor called the radical delocalization value and the intrinsic stability via a previously established bond dissociation enthalpy model. The thiadiazinyl radical was chosen as case study of this new approach of inverse design in stable radical chemistry. The resulting optimal structure is found to be highly stable, intrinsically more than other well-known stable radicals, like verdazyls and N,N-diphenyl-N′-picrylhydrazyl, and even rivaling the intrinsic stability of nitrogen monoxide.

Introduction

As free radicals are molecules with an unpaired electron, they are considered as highly unstable species, willing to react quickly with other compounds to capture that *missing* electron and gain stability. However, there exist many radicals with sufficiently long

Correspondence to: Freija De Vleeschouwer, fdevlees@vub.ac.be.

Supporting Information Available

Geometries in Cartesian coordinates and computed total energies (with indication of the computational method used) of the main structures. This material is available free of charge via the Internet at http://pubs.acs.org.

lifetimes to be observed experimentally or even isolated as pure compounds, and many applications in synthesis (oxidation catalysts, living radical polymerization), materials science (magnetochemistry, battery components) and biochemistry and medicine (spin labeling, EPR imaging, redox biochemistry) take advantage of this particular property. For a detailed overview of stable radical chemistry, we refer to the books by Forrester, Hay, and Thomson [1] and, more recently, Robin G. Hicks. [2] Nowadays, numerous families of stable radicals are known, in which the molecular architecture provides the grounds for the higher stability. This higher stability can be achieved in several ways, inducing, however, small differences in the definition of stability. First of all, steric protection through the incorporation of bulky substituents around the radical center(s) provides kinetic and, to a lesser degree, thermodynamic stability to an otherwise reactive system. [3] However, this kinetic stabilization effect can be of such an order that it will completely prevent the radical system from interacting with its environment, while many of the applications in stable radical chemistry require some interaction. An alternative approach to stabilize radicals, more related to thermodynamic stability, is try to delocalize the spin over multiple atomic centers (so-called π-radicals), which is generally recognized to be an effective way to reduce the reactivity of the system. In addition, it is known that many of the most stable radicals have a heteroatomic radical center, such as nitrogen, oxygen or sulfur. A well-chosen combination of all those ingredients stands for the perfect recipe to design in a rational way new stable radicals, as is demonstrated by the large number of stable radicals that were synthesized in the past decades. [2]

In literature little can be found on the theoretical design of stable radicals. In this work, we will for the first time apply inverse design to find new radicals with a high stability. The design of molecules with optimal properties is an important challenge in chemistry because of the astronomically large number of possible stable structures that is accessible in chemical space. As an example, consider a certain molecular framework where the substituents on, for instance, 10 sites are allowed to be altered. A library of just 10 substituents that may appear at any of the 10 different sites within the molecular framework of interest gives already rise to a database of 10 billion chemical structures, although not all of them may be stable. This obstacle can be overcome through inverse molecular design. In inverse design [4–11] one uses the computation of certain (reactivity) descriptors to design molecules with an optimal property. In this case, the property that needs to be optimized is radical stability, but which marker can be used to describe this vague concept? Theoreticians, for obvious reasons, cannot use the practical “put it in a bottle” definition of experimentalists. Therefore we turn to the concept of intrinsic stability, of which a rough initial definition was given by Coote *et al.* [12]: “a measure of the general propensity of a radical to react across a range of different chemical environments”. In 2008, we introduced a model to obtain intrinsic radical stabilities from the computation of the bond dissociation enthalpy (BDE) of molecules and by using only chemical concepts of the individual radical fragments. [13] In this model, combinations of the radicals with different chemical environments were considered, leading to a radical stability scale that can be regarded as practically intrinsic. This model has been used not only to measure the stability of small monoradicals, but also has proven its value in i.e. determining the stability of large polyaromatics [14] and biradical systems [15], and even in explaining the regioselectivity of radical addition reactions. [16] In the context of this study, intrinsic stability is related primarily to thermodynamic stability, as it is identified with electronic stabilization effects and is irrespective of the environment or reaction partner. We would like to stress, however, that stability is not the same as reactivity, as reaction mechanisms are not solely driven by the stability of the reaction partners.

This work covers the search of stable radicals through the optimization of two different properties, a newly introduced descriptor called the radical delocalization value (*RDV*) and

the intrinsic stability via a previously presented BDE model. [13] Hence, the focus lies predominantly on thermodynamic stabilization effects. We have chosen the thiadiazinyl radical system as case study of this new approach of inverse design in stable radical chemistry. The stability of the resulting optimal structure will be compared to the intrinsic stability of already synthesized thiadiazinyl radicals, as well as other well-known stable radicals, like triphenylmethyl, phenalenyl, verdazyl and hydrazyl.

Results and Discussion

Thiadiazinyl radical system

In this work, we will start the design of new stable radicals based on the thiadiazinyl radical template, as depicted in Figure 1. The structure consists of two joined six-membered rings, of which one ring contains a sulfur atom accompanied by two nitrogen atoms. The unpaired electron is delocalized and the two nitrogen atoms are the potential reactive radical centers (see Figure 1), having only a slightly higher spin density (0.327 for the upper nitrogen; 0.319 for the lower nitrogen) than the sulfur atom (0.291). Less than a decade ago, Kaszynski *et al.* were able to synthesize five different thiadiazinyl radicals, all of them with a phenyl group on the carbon atom in between the two nitrogen atoms; their structures are shown in Figure 2. [17;18] Most of these structures are found to be persistent in toluene solutions at very low temperatures, whereas the Ph_F and Ph_Cl derivatives are even stable enough to be isolated. Kinetic data have shown that Ph_F has a half-life in solution of about 4 months in the absence of air and that Ph_Cl decomposes quickly in the presence of oxygen with a half-life of about 40 min. Both radicals were found to be sufficiently stable for chromatographic isolation and vacuum sublimation. Considering the fact that their structures are nearly planar, these radicals seem suitable to construct structural elements of liquid crystals. [19]

Remarkably enough, computational studies by Kaszynski *et al*. [17] indicate that the spin distributions in thiadiazinyl radicals are concentrated on the nitrogen atoms and the sulfur atom with only a modest amount of spin delocalization on the adjacent aromatic ring. This makes the thiadiazinyl radical our ideal case study: it has an interesting architecture with heteroatomic radical centers and possibly enhanced delocalization over the adjacent ring, depending on the type of substituents on that ring. The scope of this work is to find the most stable thiadiazinyl radical among a whole set of derivatives through inverse design, by changing substituents on sites that can be modified within the molecular framework in Figure 1 in such a way that with every step a more stable derivative is found. We will use the discrete best-first-search (BFS) method to optimize the stability of the thiadiazinyl radical derivatives, of which the working scheme is already described in detail in previous works [20;21]. In summary, the BFS method uses an algorithm that makes structural modifications while evaluating the impact of those changes on the property of interest. In the implementation of the independent site approximation, the variable sites are presumed independent of each other and are optimized individually through a sequential search and selection of the most favorable substituent for the target property. In our particular case, there are five sites that can be adjusted, one in the ring with the heteroatoms and four in the adjacent ring. Our database of substituents is a mix of electron-withdrawing and electron-donating functional groups (both inductively as by resonance) and consists of the following 21 possibilities: (C)-$NHCH_3$, (C)-$SOCH_3$, (C)-OCH_3, (C)-SCH_3, (C)-SO_3H, (C)-COOH, (C)-CF_3, (C)-CH_3, (C)-CHO, (C)-CFO, (C)-OOH, (C)-SOH, (C)-NH_2, (C)-OH, (C)-SH, (C)-CN, (C)-H, (C)-F, (C)-Cl, (C)-Br and (N), where the atom in parenthesis refers to the atom placed in the ring. Bulky substituents, like for instance the phenyl and *tert*-butyl groups, were deliberately left out for two reasons: 1) the objective of this study is to focus on thermodynamic stability, while bulky groups would enhance predominantly the kinetic stability; 2) the inclusion of very bulky functional groups would make the method clearly

more difficult to implement, which would cause an non-negligible increase in computational time.

Delocalization Value

One of the main approaches to increase the thermodynamic stability of a π-radical is delocalization of the spin over several atomic centers. Therefore we introduce a new descriptor, the radical delocalization value *RDV*, that is based on the computed spin densities $\rho_{S,i}$ on the heavy atoms *i* in the radical system:

$$RDV = \sum_{i=1}^{A} \left(f\left(\rho_{S,i}\right) \right)^2 \quad \text{with } f\left(\rho_{S,i}\right) = \begin{cases} \rho_{S,i} & \text{if } \left|\rho_{S,i}\right| \geq 0.05 \\ 0 & \text{otherwise} \end{cases} \quad (1)$$

It is defined as the sum of the squared spin densities that – in absolute value – are bigger than the threshold of 0.05. This boundary condition (BC) is, though somewhat arbitrary, based on our experience with reactivity indices and is included to identify at the same time the number of heavy atoms that contribute to the delocalization of the spin. Including all spin densities will have only a minor effect on *RDV*, since taking the square of small values ($|\rho_{S,i}| < 0.05$) would introduce only a tiny contribution. The smaller is the total value of this delocalization quantity, the more the radical system is delocalized. We want to remark that this index might fail when negative values for the spin density are too large.

In the first inverse design approach toward the most stable thiadiazinyl radical, the BFS procedure was used with the radical delocalization value taken as the property to be optimized; in other words, the delocalization of the unpaired electron was taken as the determining factor to find the most stable radical. During the property optimization, the geometry of each constructed thiadiazinyl derivative was optimized (using the UB3LYP/6–31G(d) computational method). However, because of computational cost limitations, during the property optimization no frequency calculations were performed to check whether the structure is a real minimum on the potential energy surface, no conformational analysis was incorporated and possible tautomerism was not checked.

Full convergence of the BFS process was reached within 4 global iterations, going through all sites and substituents. In total 361 structures had to be computed, which is a negligible amount compared to the size of the investigated chemical space, namely $M^N = 5^{21} \approx 5\ 10^{14}$ with *M* the number of sites and *N* the number of substituents. Figure 3 clearly shows for all constructed structures the correlation between the number of heavy atoms (in percentage) that participate in delocalizing the unpaired electron over the thiadiazinyl radical system and the radical delocalization value, demonstrating the viability of the *RDV* definition.

The resulting optimum (RDV_open_ring) is shown in Figure 4a, with an *RDV* value of 0.146, considerably lower than the *RDV* values for the thiadiazinyl reference radical, Ph_F and Ph_Cl (see Table 1). Including the spin densities on all atoms of the system in the definition of *RDV* (BC = 0.00 in Eq. 1) augments the original *RDV* values only with a tiny amount, as can be seen from Table 1. Although a high spin delocalization is observed, the RDV_open_ring structure is not expected to be very stable. In this derivative the ring structure present in the framework of the thiadiazinyl radical system is broken up, leaving an azide ending that can easily lose two nitrogen atoms.

The first structure, encountered during the *RDV* optimization that does not contain the azide group is shown in Figure 4b and has an *RDV* value of 0.188, which is still considerably less than the reference thiadiazinyl radical. The spin densities for all five structures in the list are depicted in Figure 5 using color-coding. In the RDV_closed_ring structure, the ring

containing the nitrogen and sulfur atoms is retained, with a peroxide group on carbon site 1 in between the two nitrogen atoms. The extra stabilization through hydrogen bonds between, firstly, the hydrogen of the peroxide group and the bottom nitrogen, and, secondly, the hydrogen atoms of the two $HNCH_3$ groups and the oxygen atoms of the carboxyl group on the adjacent ring, together with an enhanced spin delocalization over the adjacent ring promises a clear improvement in intrinsic stability compared to the thiadiazinyl reference system.

To check this expectation, we have computed the intrinsic stabilities from a bond dissociation enthalpy (BDE) model, which was introduced in 2008. [13] The model breaks down BDEs into parts that (only) incorporate intrinsic properties of the radical fragments, like radical stability (*stab*), electrophilicity (ω), and Pauling electronegativity (χ):

$$BDE(A-B)=\begin{cases} (stab_A+stab_B)+a\Delta\omega_A\Delta\omega_B, & \text{if } \Delta\chi_A<0 \text{ and } \Delta\chi_B<0 \\ (stab_A+stab_B)+a\Delta\omega_A\Delta\omega_B+b\Delta\chi_A\Delta\chi_B, & \text{otherwise} \end{cases} \quad (2)$$

The enhanced Pauling electronegativity of the radical centers $\Delta\chi$ can be obtained simply as $\Delta\chi = \chi - 3$, with $\chi = 3$ as the boundary between strongly and weakly electronegative radical centers. Pauling's electronegativity scale was constructed using a large set of bond dissociation enthalpies and by applying the following formula: [22]

$$\chi_A-\chi_B=(\text{eV})^{-\frac{1}{2}}\sqrt{BDE(A-B)-\frac{BDE(A-A)+BDE(B-B)}{2}} \quad (3)$$

The electronegativity of the fluorine atom was chosen as a reference and set to a value of 4.0. The enhanced electrophilicity index $\Delta\omega$ is defined as the difference between the electrophilicity index ω, as introduced by Parr et al, [23] and the borderline between electrophilicity and nucleophilicity for radicals, which is situated around 2 eV ($\Delta\omega = \omega - 2$). This borderline was the result of a comparison of our previously introduced radical electrophilicity scale with other classifications from literature concerning the electrophilic or nucleophilic behavior of radicals. [24] Finally, the parameters *a* and *b* were estimated previously to be −12.69 kJ mol^{-1} eV^{-2} and −218.10 kJ mol^{-1}, respectively, using a least-square fit on a BDEs training set, that consisted of the combination of 47 radicals with the radical fragments CH_2OH, H, and F. Through this least-square fit, also estimations for the intrinsic stability *stab* for those 47 radicals were obtained. More information on how the different terms in the model contribute to the BDEs can be found in detail in ref. 13. Note that the *a* and *b* parameters in this work are slightly different from the values reported in ref. 13, due to some improved BDE values in the training set. The *stab* values, however, are not affected. Some effects that are dependent on both radical fragments were not yet included in the model, like for instance steric interactions, which are anticipated to be more prominently present in the case of larger-sized radicals. Since we are investigating the rather bulky thiadiazinyl radicals, the small hydrogen atom was chosen as the reaction partner. As such, no steric repulsion is to be expected, so that the BDE model should result in an estimated stability value (*stab* in Eq. 2) that is exclusively thermodynamic of nature. The estimated intrinsic stability values *stab* for all five derivatives can be retrieved from Table 2. We want to remind that the lower is the value of the property *stab*, the more stable is the radical system. The RDV_closed_ring structure is indeed found to be intrinsically the most stable. However, although a trend shows up, there does not seem to be enough correlation between the radical delocalization value and the intrinsic stability to state with confidence that *RDV* is the ideal property to model thermodynamic stability and therefore to be sure that

RDV_closed_ring is the ultimate stable thiadiazinyl radical in our predefined chemical space. For that reason a second inverse design approach was executed, now with the intrinsic stability *stab* as the property to be optimized.

Intrinsic Stability Through the BDE Model

As can be seen from Eq. 2, full calculation of the property *stab* requires a lot of computational time, especially since for each step, i.e. every substituent on every site, the hydrogen atom can be attached to two possible radical centers (the two nitrogen atoms in Figure 1) and there is no way to know in advance which will be the most stable compound. As a consequence, for every step three geometry optimizations, three frequency calculations and five single point calculations are needed. This would be computationally too demanding, even when the BFS procedure is used. Therefore some rational approximations were made: 1) the electrophilicity term in Eq. 2 was set to zero, as the $\Delta\omega$ value of H is 0.063 eV resulting in a estimated maximal error on *stab* of around 2 kJ mol^{-1}; 2) the sum of zero point vibrational energies and thermal corrections to the enthalpy is taken as a constant because of the similar values observed for the structures in Table 1 (in this case −29.2 kJ mol^{-1}) resulting in an estimated error on *stab* of only a few kJ mol^{-1}. Rewriting Eq. 2 with the inclusion of all the suggested approximations leads to the following model:

$$BDE(R-H)=(E_R-1361.4-E_{R-H})-29.2=(stab_R+235.7)+8.7 \quad (4)$$

with R the thiadiazinyl radical derivative and E_H = −1361.4 kJ mol^{-1}, $stab_H$= 235.7 kJ mol^{-1} and $b\Delta\chi_R\Delta\chi_H$ = 8.7 kJ mol^{-1}. Using Eq. 4 implies that for each step only three geometry optimizations (R, R[N1]-H and R[N2]-H) and two single point calculations are required, which is computationally much more feasible. Convergence was reached within 3 global iterations, meaning that only 281 structures had to be constructed on a chemical space size of around half a quadrillion possible structures.

The resulting optimum is depicted in Figure 6 as Thiadiazinyl_opt and has a *stab* value of only 13.1 kJ mol^{-1}. Although the structure looks rather similar to the *RDV* optimum in Figure 4b, there is a large improvement (of almost 40 kJ mol^{-1}) in intrinsic stability, while the radical delocalization values are not so different (the *RDV* of Thiadiazinyl_opt is 0.213). Delocalization of the unpaired electron certainly plays a role but it does not seem to be the only stabilizing effect. To get an idea about the influence each substituent on a particular site has on the property *stab*, a 3-D plot was included in Figure 7 covering all the structures that were constructed during the last global iteration cycle.

For every site, it can be easily seen which functional groups will result in a similar *stab* value. For example, substituting the thiol group on site 5 with e.g. chlorine, bromine or a methylamino group, or by putting a nitrogen atom in the ring will hardly alter the value of *stab*. In addition, the more the peaks (for a given site) vary in height, the more important the optimal substituent and therefore in some way also that particular site is to obtain a more stable system. However, we need to keep in mind that we cannot make definitive conclusions about the impact of every substituent on every site, even though we applied the independent site approximation. It is clear from the 3-D plot in Figure 7 that site 5 shows the smallest variations between the different substituents. This is confirmed by the data in Table 3.

Both the average and the median of *stab* are below 20 kJ mol^{-1} for site 5, with a maximal *stab* difference of 30.5 kJ mol^{-1} for the whole set of substituents on that site. Out of 20 structures, 12 have a *stab* value within 10 kJ mol^{-1} of the optimum and 18 within 20 kJ mol^{-1}, indicating that this site has a minor influence on the intrinsic stability of the thiadiazinyl system. Considering site 1, we found that more than half of the substituents

generate a structure for which the *stab* value is less than 20 kJ mol^{-1} away from the optimal value, so also site 1 has a limited influence. Sites 2, 3 and 4 seem to have the biggest impact: site 2 and site 4 for having almost no structures with a *stab* value close enough to the optimum and site 3 for being a mix between structures that have either a relatively low or a relatively high intrinsic stability. However, only the methylamino group on site 4 is clearly participating in stabilizing the π-radical through the overlap of *p*-orbitals, which is supported by both the spin densities and the bond lengths. Other functional groups on site 4 resulting in structures for which about the same intrinsic stability was estimated as the optimum, like (C)-OH and (C)-NH_2, share that same mesomerically electron-donating ability. Therefore we can state that placing a mesomerically electron-donating functional group on site 4 is important to obtain a highly stable thiadiazinyl radical.

As mentioned above, the optimal structure Thiadiazinyl_opt is certainly a lot more stable than the reference thiadiazinyl radical, but how stable is this system compared to other well-known radical systems? Figure 8 depicts five of the most common stable radicals, namely triphenylmethyl, [25] phenalenyl, [26] N,N-diphenyl-N′-picrylhydrazyl, [1] 1,5-diphenylverdazyl (Verdazyl_H), 1,3,5-triphenylverdazyl (Verdazyl_Ph). [27] Triphenylmethyl owes its stability (or more precisely its persistency) largely to the three bulky phenyl groups, resulting in steric protection of the central carbon atom. Its stability has therefore more kinetic origin. Phenalenyl, on the other hand, demonstrates perfectly the effect of electron delocalization on stability and its stability is therefore thermodynamic of nature. N,N-diphenyl-N′-picrylhydrazyl is an indefinitely stable radical and has been used as an EPR reference compound for decades, while verdazyl radicals are the only class of radicals with stability rivaling that of the nitroxides. Table 4 comprises the computed intrinsic radical stabilities *(stab)*, using Eq. 2 and the hydrogen atom as reaction partner, for a set of eleven radical systems, including the reference thiadiazinyl radical, the synthesized thiadiazinyl radical derivatives Ph_F and Ph_Cl, the *stab* optimum Thiadiazinyl_opt and its very close derivatives Thiadiazinyl_opt_OH[28] (most stable derivative during the BFS optimization that does not have a (possibly too reactive) peroxide group on site 1) and Thiadiazinyl_opt_Ph (to introduce a more bulky substituent close to the radical center outside the list of substituents used) as depicted in Figure 6 and finally the five known stable radical systems as described above.

Our optimum is found to be intrinsically the most stable radical system, followed closely by its derivative Thiadiazinyl_opt_OH and phenalenyl and the slightly less stable verdazyl radicals. The triphenylmethyl and N,N-diphenyl-N′-picrylhydrazyl radicals are found to be intrinsically the least stable among the eleven investigated structures. When these results are compared against our previously established radical stability scale [13], only 5 out of 47 other radicals fit into the range outlined by the *stab*[H] values in Table 4: tosyl and phenylsulfonyl (70.7 kJ mol^{-1}), NF_2 (65.8 kJ mol^{-1}), NO_2 (61.7 kJ mol^{-1}), phenoxy (34.4 kJ mol^{-1}) and the most stable of the scale, NO (5.9 kJ mol^{-1}). Remark that this thermodynamic stability definition (*stab*[H]) indeed separates those radical systems that are stable through electronic effects from those that are stable mainly because of steric protection of the radical center. In order to get a better idea about the latter effect, namely the kinetic stability of these radical systems, we have computed the radical stability *stab*, now using the methyl radical (*stab*[CH_3]) and the *tert*-butyl radical (*stab*[t-Bu]) as reaction partners in Eq. 2. Because the model in Eq. 2 contains no term describing the steric interaction between two radical fragments, this term will be incorporated in the value for the quantity *stab*. Going from H to CH_3 as a reaction partner, a huge decrease in the *stab* value is noted for Ph_F, Ph_Cl and especially N,N-diphenyl-N′-picrylhydrazyl with a decrease of 85.5 (!) kJ mol^{-1}. The latter has now become even more stable than the verdazyl radicals. The stability of the phenalenyl radical is affected the least with a decrease of only 11.9 kJ mol^{-1}. The influence of the bulky substituents around the radical center is even more visible

when the larger *tert*-butyl is taken as the reaction partner. Going from H to *t*-Bu, the N,N-diphenyl-N′-picrylhydrazyl radical is now 181.9 kJ mol^{-1} more stable than before.

Also the stability of the triphenylmethyl radical improves greatly with a *stab* decrease of 124.1 kJ mol^{-1}. The smallest decreases are observed for phenalenyl (36.4 kJ mol^{-1}) and Verdazyl_H (26.5 kJ mol^{-1}), demonstrating the effect of the extra phenyl group in Verdazyl_Ph as a steric protector (decrease of 62.0 kJ mol^{-1} in *stab*). The thiadiazinyl radical derivatives are not influenced in the same way by the change of reaction partner and the origin of this behavior is not clear. The effect of steric protection by the bulky phenyl group cannot be the only explanation, as a similar decrease is found for Ph_F, Ph_Cl and Thiadiazinyl_ref, as well as for Thiadiazinyl_opt, Thiadiazinyl_opt_OH and Thiadiazinyl_opt_Ph. Nevertheless, we can state that the difference between *stab*[*t*-Bu] and *stab*[H] gives a measure for the steric protection of the radical center and therefore an approximate measure for the kinetic stabilization of the radical system.

Computational Details

All calculations were performed within the Kohn-Sham framework, using the Gaussian 09 software package. [29] During the inverse design search, all geometries were optimized at the (U)B3LYP/6–31G(d) level of theory. [30] The Natural Population Analysis (NPA) [31] partitioning scheme was used to obtain the spin densities on all the atoms of the system at the UB3LYP/6–31G(d) level of theory.

The electrophilicity index is defined as: [23]

$$\omega=\frac{\mu^2}{2\eta} \quad (5)$$

with $\mu$the electronic chemical potential and η the chemical hardness. For an *N-electron* system with external potential v(**r**) and total energy *E*, the electronic chemical potential μ is defined as the partial derivative of the energy to the number of electrons at constant external potential: [32]

$$\mu=\left(\frac{\partial E}{\partial N}\right)_{v(\mathbf{r})}\approx-\frac{I+A}{2} \quad (6)$$

where *I* and *A* are the vertical ionization energy and electron affinity, respectively. Parr and Pearson [33] proposed the following definition for the chemical hardness η differentiating the chemical potential to the number of electrons, again at constant external potential:

$$\eta=\left(\frac{\partial^2 E}{\partial N^2}\right)_{v(\mathbf{r})}\approx I-A \quad (7)$$

Throughout this work, the two quantities *I* and *A*, and therefore the electrophilicity index ω, were calculated as an energy difference between the neutral and the cation or the anion, respectively, using the B3LYP/6–311+G**method.

The bond dissociation enthalpies *[BDE]* in Eq. 2, or the electronic energies (*E*) in Eq. 4, were computed from single point calculations with the B3P86 functional [34] and basis set 6–311+G**. In a previous paper [13], a comparative study with experiment was performed

involving 89 BDEs and it was concluded that the B3P86 functional performs much better than B3LYP (mean absolute deviation of 10.5 and 24.1 kJ/mol, respectively) in calculating this quantity.

For the main structures, listed in Table 4, the geometries were optimized with a higher basis set, namely 6–311+G** instead of 6–31G*. Subsequent frequency calculations at the same level (B3LYP/6–311+G**) provided the thermal corrections to the enthalpy. All energy calculations were then performed with the methods as listed above ((U)B3LYP/6–311+G** for the electrophilicity index and (U)B3P86/6–311+G** for the BDEs). For the computation of the electrophilicity of the hydrogen atom, extra diffuse functions were added to the basis set, so the B3LYP/6–311++G** level of theory was used.

Conclusions

The inverse design approach combined with the best-first-search methodology resulted in an intrinsically highly stable thiadiazinyl radical, and this in an effective way as less than 400 structures needed to be constructed in a chemical space of nearly half a quadrillion derivatives. The intrinsic stability of the optimal thiadiazinyl radical, which is thermodynamic of nature, was obtained via a previously established bond dissociation enthalpy (BDE) model with the hydrogen atom as reaction partner. The optimum is more than 40 kJ mol^{-1} more stable than the isolable thiadiazinyl radicals, synthesized by Kaszynski *et al*. Remark, however, that the intrinsic stability value does not predict straightforwardly the reactivity of the system, as reactivity is not only governed by the stability of the reaction partners. The intrinsic stability of the optimal structure even surpasses that of the well-known stable verdazyl and N,N-diphenyl-N′-picrylhydrazyl radicals and, moreover, approaches the intrinsic stability of nitrogen monoxide, the most stable radical we have encountered so far. We found that sites 1 and 5 only have a minor influence on the stability, while the impact of sites 2, 3 and 4 is much more essential. More particularly, we observed that placing a mesomerically electron-donating functional group on site 4 seems to be crucial to obtain a highly stable thiadiazinyl radical. In addition we computed for all key radicals two extra stability values using the same BDE model but now with the larger methyl and *tert*-butyl radicals as reaction partners. These latter values give an insight into the effect of kinetic stabilization through the steric protection of the radical center by the incorporation of bulky substituents. We found that the much higher stability of certain radicals can indeed be traced back to the kinetic stabilization of the radical system. Therefore we conclude that the BDE model can evaluate both the thermodynamic and the kinetic stability through the calculation of only two properties. Together with the inverse design approach we have established a rational as well as an easy way to obtain highly stable radicals in predefined chemical spaces on a theoretical basis. The present approach might open new doors to the systematic development of new radical systems with exceptional stability.

Supplementary Material

Refer to Web version on PubMed Central for supplementary material.

Acknowledgments

F. D. V. acknowledges the Research Foundation-Flanders (FWO) for a postdoctoral fellowship. W. Y. thanks the NIH for support of the UPCMLD (P50-GM067082) and the NSF (CHE-09–11119). F. D. P. and P. G. acknowledge the Fund for Scientific Research-Flanders (FWO) and the Free University of Brussels for continuous support to their research group.

References

1. Forrester, AR.; Hay, JM.; Thomson, RH. Organic Chemistry of Stable Free Radicals. Academic Press; London: 1968.
2. Hicks, RG. Stable Radicals: Fundamentals and Applied Aspects of Odd-Electron Compounds. John Wiley & Sons Ltd; Chichester, UK: 2010.
3. Power PP. Chem Rev. 2003; 103:789. [PubMed: 12630853]
4. Ert P. J Chem Inf Comput Sci. 2003; 43:374. [PubMed: 12653499]
5. Lipinski C, Hopkins A. Nature. 2004; 432:855. [PubMed: 15602551]
6. Dobson CM. Nature. 2004; 432:824. [PubMed: 15602547]
7. Weiss GA. Curr Opin Chem Biol. 2007; 11:241.
8. Kuhn C, Beratan DNJ. Phys Chem. 1996; 100:10595.
9. Wang ML, Hu X, Beratan DN, Yang JW. Am Chem Soc. 2006; 128:3228.
10. Jòhannesson GH, Bligaard T, Ruban AV, Skriver HL, Jacobsen KW, Nørskov JK. Phys Rev Lett. 2002; 88:255506. [PubMed: 12097098]
11. von Lilienfeld OA, Lins RD, Rothlisberger O. Phys Rev Lett. 2005; 95:153002. [PubMed: 16241723]
12. Coote ML, Dickerson AB. Aust J Chem. 2008; 61:163.
13. De Vleeschouwer F, Van Speybroeck V, Waroquier M, Geerlings P, De Proft FJ. Org Chem. 2008; 73:9109.
14. Hemelsoet K, De Vleeschouwer F, Van Speybroeck V, De Proft F, Geerlings P, Waroquier M. Chem Phys Chem. 2011; 12:1100. [PubMed: 21438107]
15. De Vleeschouwer, F.; De Proft, F.; Geerlings, P. Invited contribution to J. Mol. Struct. (THEOCHEM). In: Chattaraj, PK.; Thakkar, AJ., editors. Special issue on Conceptual DFT. Vol. 943. 2010. p. 94
16. De Vleeschouwer F, Jaque Olmedo P, Geerlings P, Toro-Labbé A, De Proft F. J Org Chem. 2010; 75:4964. [PubMed: 20614876]
17. Zienkiewicz J, Kaszynski P. J Org Chem. 2004; 69:7525. [PubMed: 15497978]
18. Kaszynski P. Molecules. 2004; 9:716. [PubMed: 18007472]
19. Zienkiewicz J, Fryszkowska A, Zienkiewicz K, Guo F, Kaszynski P, Januszko A, Jones D. J Org Chem. 2007; 72:3510. [PubMed: 17407358]
20. Balamurugan D, Yang W, Beratan DN. J Chem Phys. 2008; 129:174105. [PubMed: 19045331]
21. De Vleeschouwer F, Yang W, Beratan DN, Geerlings P, De Proft F. Phys Chem Chem Phys. 2012; 14:16002. [PubMed: 23089917]
22. (a) Pauling L. J Am Chem Soc. 1932; 54:3570.(b) Pauling, L. The Nature of the Chemical Bond and the Structures of Molecules and Crystals. 3. Cornell University Press; Ithaca, NY: 1960.
23. Parr RG, Von Szentpaly L, Liu SB. J Am Chem Soc. 1999; 121:1922.see also the review: Chattaraj PK, Sarkar U, Roy DR. Chem Rev. 2006; 106:2065. [PubMed: 16771443]
24. De Vleeschouwer F, Van Speybroeck V, Waroquier M, Geerlings P, De Proft F. Org Lett. 2007; 9:2721. [PubMed: 17559221]
25. Gomberg M. J Am Chem Soc. 1900; 22:757.
26. (a) Reid DH. Tetrahedron. 1958; 3:339.(b) Sogo BP, Nagazaki M, Calvin M. J Chem Phys. 1957; 26:1343.
27. Kuhn R, Trischmann H. Angew Chem Int Ed Engl. 1963; 3:155.
28. The Thiadiazinyl_opt_OH structure (or 3-hydroxybenzothiadiazinyl) can undergo tautomerism, which is not checked during the property optimization. Hence, we have tested whether there exists a more stable tautomer by computing the electronic energy of the two possible 3-keto tautomers of 3-hydroxybenzothiadiazinyl with the B3P86/6–311+G**//B3LYP/6–31G* computational method. We found that both tautomers are higher in energy and therefore less stable than the original 3-hydroxybenzothiadiazinyl: *E* [3-keto tautomer with H on Nl] = −1518.191274 hartree, *E* [3-keto tautomer with H on N2] = −1518.178053 hartree and *E* [3-hydroxybenzothiadiazinyl] = −1518.195268 hartree.

29. Frisch, MJ., et al. Gaussian 09, B.1. Gaussian, Inc; 2009.
30. (a) Becke AD. J Chem Phys. 1993; 98:5648.(b) Lee CT, Yang W, Parr RG. Phys Rev B: Condens Matter Mater Phys. 1988; 37:785.(c) Hehre WJ. Acc Chem Res. 1976; 9:399.
31. (a) Reed AE, Weinhold F. J Chem Phys. 1985; 83:1736.(b) Reed AE, Weinstock RB, Weinhold F. J Chem Phys. 1985; 83:735.(c) Reed AE, Curtiss LA, Weinhold F. Chem Rev. 1988; 88:899.
32. Parr RG, Donnelly RA, Levy M, Palke WE. J Chem Phys. 1978; 68:3801.
33. Parr RG, Pearson RG. J Am Chem Soc. 1983; 105:7512.
34. Perdew JP. Phys ReV B. 1986; 33:8822.

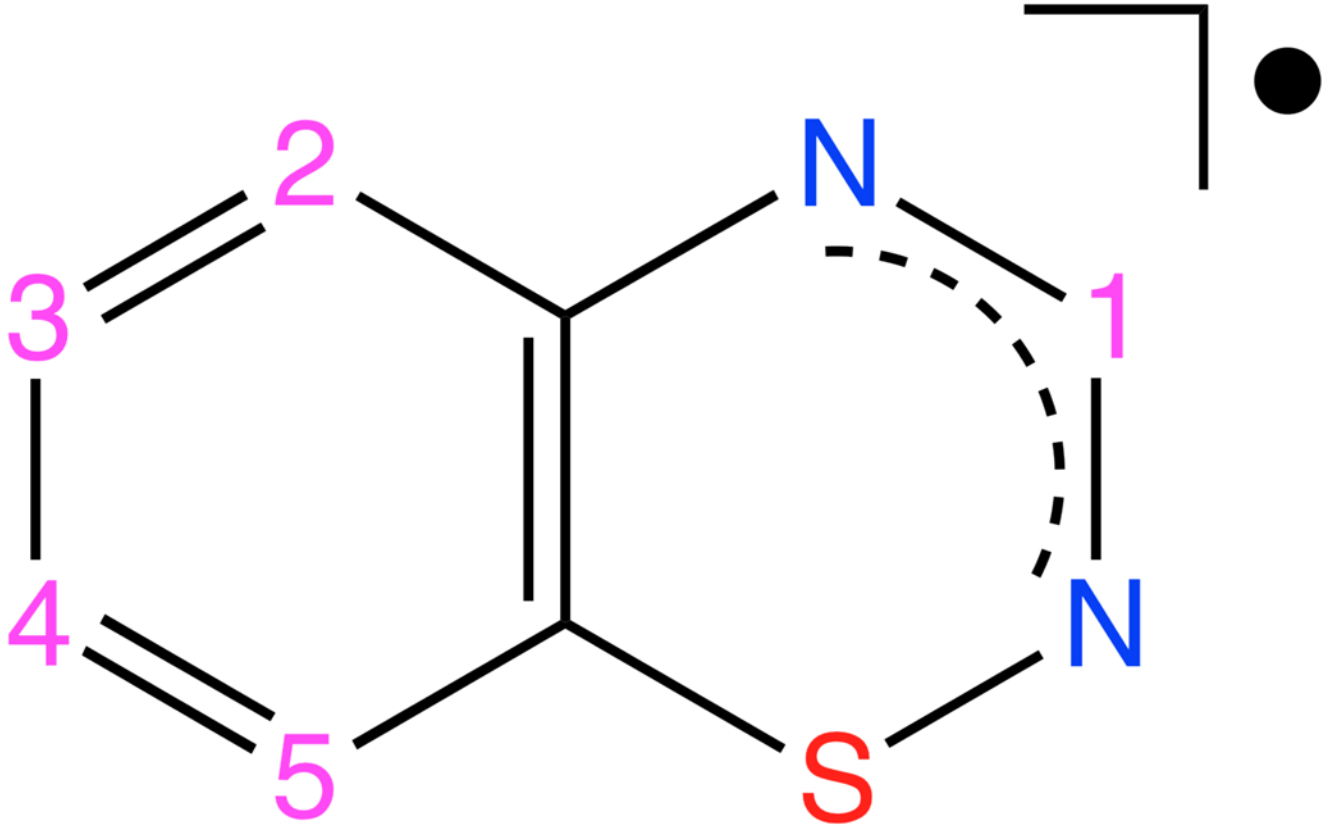

FIGURE 1.

The thiadiazinyl radical with the indication of the adjustable sites, numbered from 1 to 5, with 21 possible substituents: (C)-$NHCH_3$, (C)-$SOCH_3$, (C)-OCH_3, (C)-SCH_3, (C)-SO_3H, (C)-COOH, (C)-CF_3, (C)-CH_3, (C)-CHO, (C)-CFO, (C)-OOH, (C)-SOH, (C)-NH_2, (C)-OH, (C)-SH, (C)-CN, (C)-H, (C)-F, (C)-Cl, (C)-Br,(N).

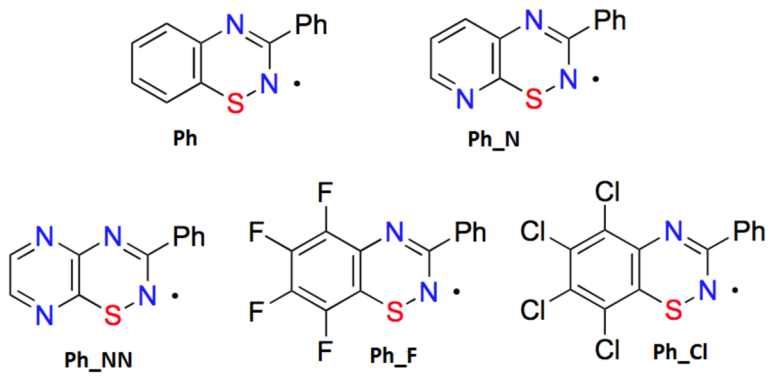

FIGURE 2.
Five thiadiazinyl radical derivatives that were synthesized by Kaszynski *et al*.[17] in 2004.

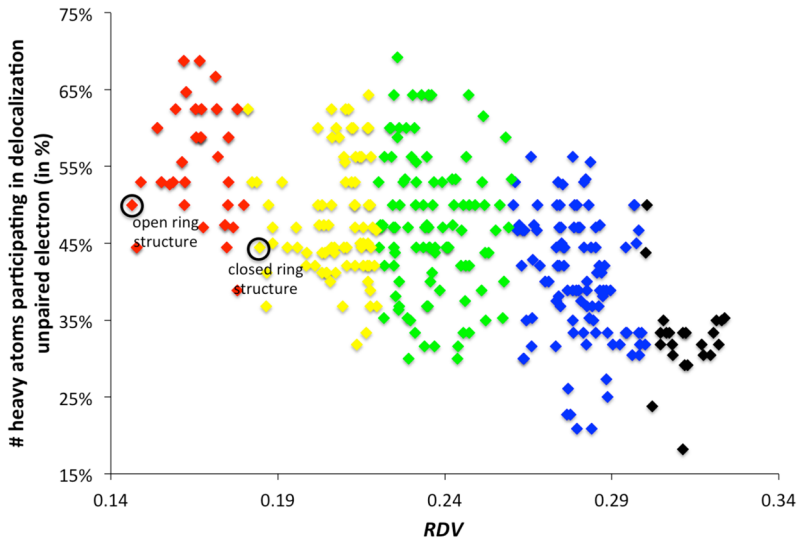

FIGURE 3.

Correlation between the number of heavy atoms (in percentage) that participate in delocalizing the unpaired electron over the thiadiazinyl radical system and the radical delocalization value (*RDV*); the color scheme and the partitioning into regions were chosen to improve transparency.

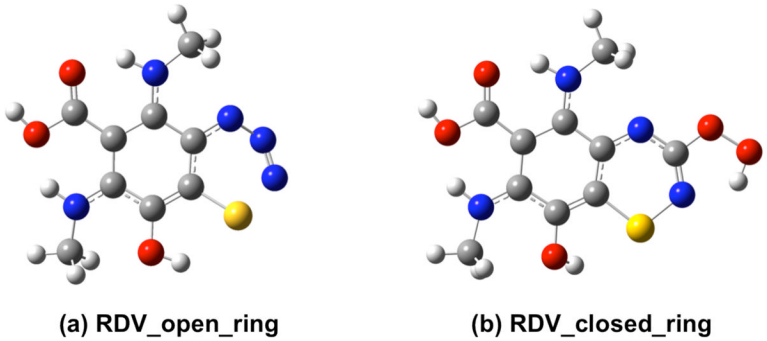

FIGURE 4.

The optimal thiadiazinyl radical derivatives, resulting from the radical delocalization value BFS optimization: (a) structure where the six-membered ring containing the radical center has broken up (*RDV* = 0.146), (b) structure where the six-membered ring containing the radical center is retained (*RDV*= 0.188); the color-coding is as follows: white: H, grey: C, blue: N, red: O, yellow: S.

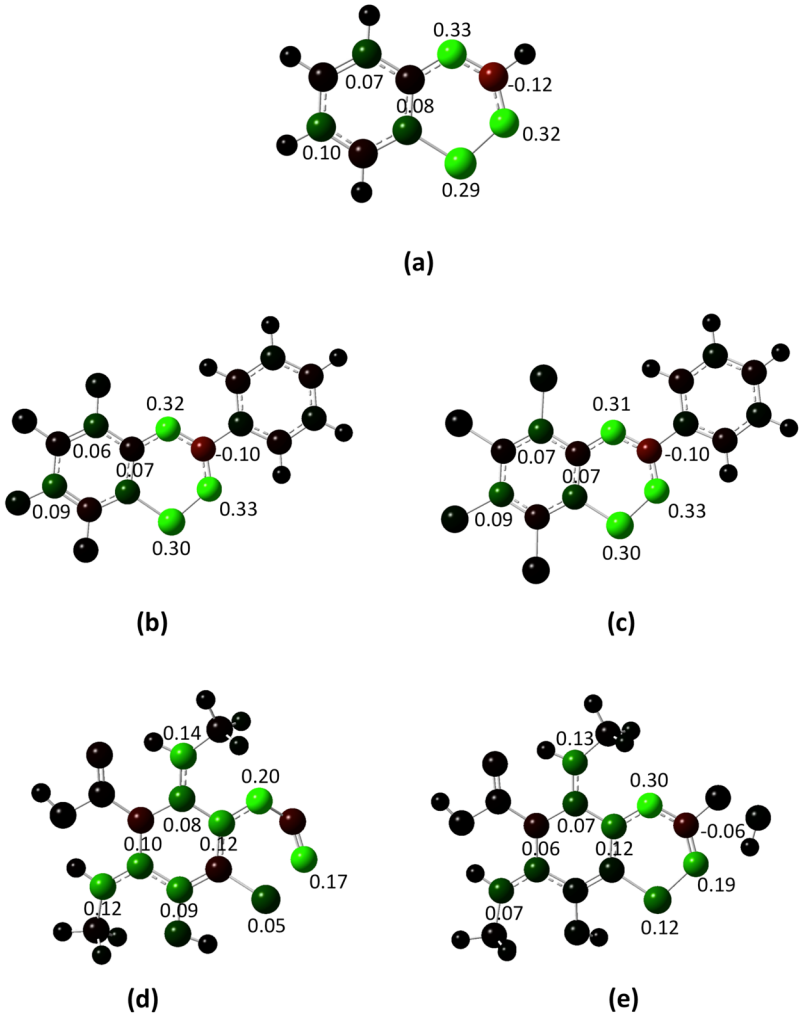

FIGURE 5.

Spin densities for a set of thiadiazinyl radical derivatives: (a) the reference thiadiazinyl radical, (b) Ph_F, (c) Ph_Cl, (d) RDV_open_ring, (e) RDV_closed_ring; the following colorcoding has been used: green for positive spin density, black for zero spin density, red for negative spin density, and the brighter the color, the higher the spin density value.

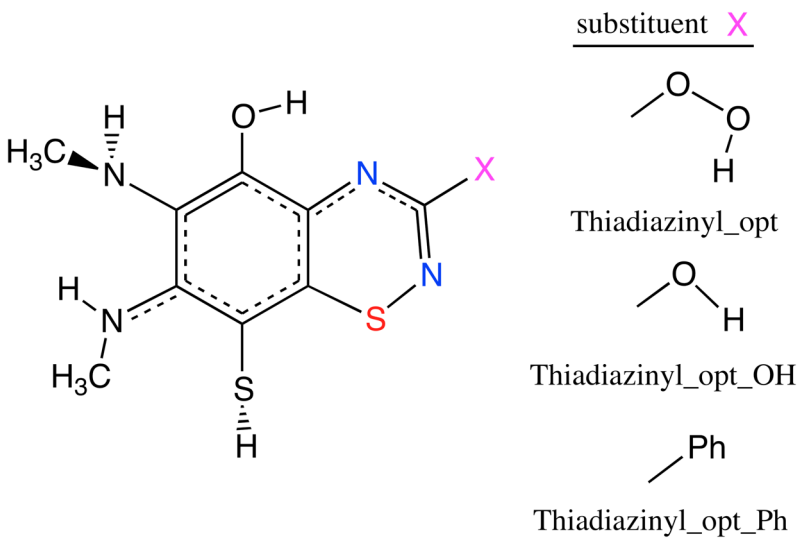

FIGURE 6.
The optimum for the intrinsic *stab* optimization (Thiadiazinyl_opt) and two other very similar derivatives (Thiadiazinyl_opt_OH and Thiadiazintl_opt_Ph).

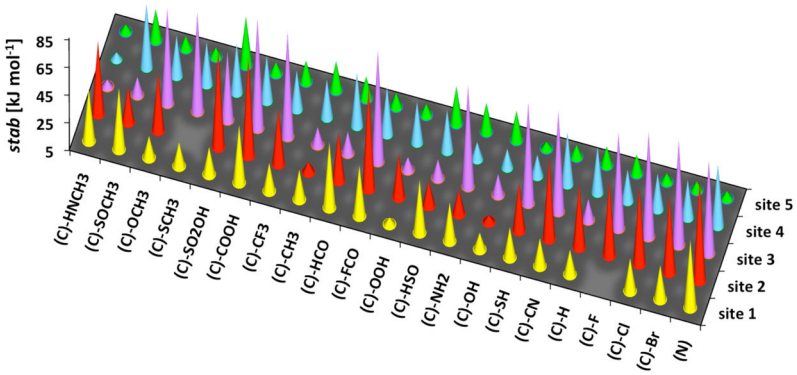

FIGURE 7.

Influence on the intrinsic *stab* value (in kJ mol^{-1}) of each substituent on a particular site for the last full iteration (until convergence).

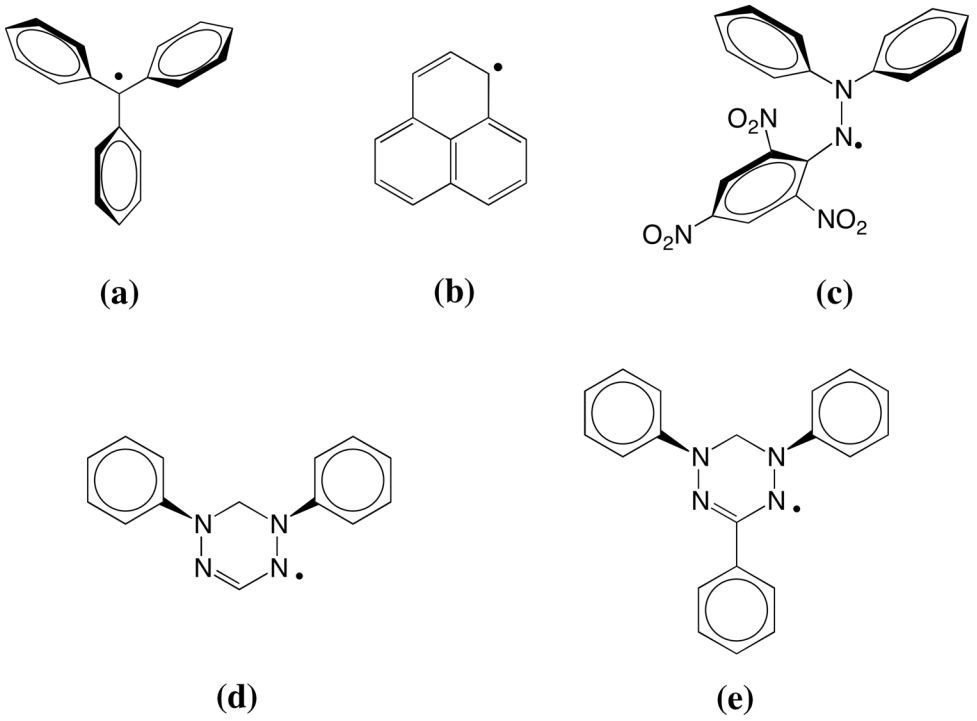

FIGURE 8.
Other well-known stable radical systems: (a) triphenylmethyl; (b) phenalenyl; (c) N.N-diphenyl-N′-picrylhydrazyl; (d) 1,5-diphenylverdazyl (Verdazyl_H); (e) 1,3,5-triphenylverdazyl (Verdazyl_Ph).

TABLE 1

Radical stabilization value (*RDV*) with boundary condition (BC) 0.05 and 0.00 (see Eq. 1) for 5 thiadiazinyl radical derivatives.

Radical	*RDV* (BC = 0.05)	*RDV* (BC = 0.00)
Thiadiazinyl_ref	0.330	0.331
Ph_F	0.328	0.331
Ph_Cl	0.317	0.320
RDV_open_ring	0.146	0.151
RDV_closed_ring	0.188	0.190

TABLE 2

Radical electrophilicity ω in eV, Pauling electronegativity χ, the bond dissociation enthalpy *BDE* between the thiadiazinyl derivative and H in kJ mol^{-1}, the intrinsic stability *stab* in kJ mol^{-1}, obtained through the BDE model (see Eq. 2 with parameters a = −12.69 kJ mol^{-1} eV^{-2} and b = −218.10 kJ mol^{-1}), for 5 thiadiazinyl radical derivatives and with H as the reaction partner.

Radical	*ω*	*X*	*BDE*	*stab*
Thiadiazinyl_ref	1.831	3.05	314.1	69.5
Ph_F	2.411	3.05	315.4	71.3
Ph_Cl	2.533	3.05	320.0	76.0
RDV_open_ring	1.968	3.05	322.3	77.9
RDV_closed_ring	1.863	3.05	297.1	52.5
H	*2.063*	*2.20*		*235.8*[a]

[a] *stab value* taken from ref. 13

TABLE 3

The average, the median, the maximum versus minimum *stab* difference (MAX_MIN) and the number of structures that are within 10 or 20 kJ mol^{-1} of the *stab* value of the optimum (Thiadiazinyl_opt) for all substituents on a particular site.

	site 1	site 2	site 3	site 4	site 5
average	32.1	48.2	54.2	33.5	18.6
median	27.9	48.5	73.8	34.5	15.0
MAX - MIN	44.2	69.1	75.7	41.3	30.5
# within 10 kJ mol^{-1} of opt.	1	1	4	2	12
# within 20 kJ mol^{-1} of opt.	11	3	7	4	18

TABLE 4

Radical electrophilicity ω in eV, Pauling electronegativity χ the bond dissociation enthalpy *BDE* between the radical system and H/CH_3/*t*-Bu in kJ mol^{-1}, the intrinsic stability *stab* in kJ mol^{-1}, obtained through the BDE model (see Eq. 2 with parameters $a = -12.69$ kJ mol^{-1} eV^{-2} and $b = -218.10$ kJ mol^{-1}), for 11 radical systems and with H/CH_3/*t*-Bu as the reaction partner.

Radical	ω	χ	*BDE*[H]	*stab*[H]	*BDE*[CH_3]	*stab*[CH_3]	*BDE*[*t*-Bu]	*stab*[*t*-Bu]
Thiadiazinyl_ref	1.831	3.05	314.1	69.5	226.9	33.6	169.2	2.3
Ph_F	2.411	3.05	315.4	71.3	214.4	15.3	174.8	−2.1
Ph_Cl	2.533	3.05	320.0	76.0	212.2	11.9	174.4	−4.6
Thiadiazinyl_opt	1.976	3.05	257.6	13.1	171.6	−23.1	132.3	−37.1
Thiadiazinyl_opt_OH	1.717	3.05	263.5	18.8	167.0	−25.1	143.4	−21.6
Thiadiazinyl_opt_Ph	1.717	3.05	276.8	32.2	190.0	−2.1	147.4	−17.6
Triphenylmethyl	1.448	2.60	318.0	81.8	233.3	48.3	113.7	−42.3
Phenalenyl	1.449	2.60	256.5	20.3	193.5	8.4	139.9	−16.1
Verdazyl_H	1.545	3.05	277.3	32.5	199.9	9.5	168.0	6.0
Verdazyl_Ph	1.614	3.05	279.0	34.3	195.5	4.4	135.5	−27.7
N N diphenyl N′ picrylhydrazyl	2.867	3.05	329.4	85.6	203.7	0.1	88.4	−96.3
H	*2.063*	*2.20*		*235.8*[a]				
CH_3	*1.209*	*2.60*				*190.6*[a]		
t-Bu	*0.651*	*2.60*						*165.5*[a]

[a] *stab* value taken from ref. 13